Pramāṇa, Vol. 24, No. 4, April 1985, pp. 545–557. © Printed in India.

Laser Raman spectroscopic study of ferroelastic $LiCsSO_4$

B RAGHUNATHA CHARY, H L BHAT, P CHANDRASEKHAR and P S NARAYANAN
Department of Physics, Indian Institute of Science, Bangalore 560012, India

MS received 13 August 1984; revised 14 December 1984

Abstract. Lithium caesium sulphate has been reported to undergo a phase transition from the room temperature orthorhombic phase with space group *P cmn* to a final phase with space group $P2_1/n$. Though a sharp anomaly in its physical properties has been found at 202°K, it was found that there was a need for careful investigations in the vicinity of 240 and 210°K. Since the changes in the crystal structure involve primarily a rotation of the SO_4 tetrahedron about the *c*-axis and as this may be reflected both in the intensity and polarisation of the internal as well as external phonon modes, the laser Raman spectra of oriented single crystals of $LiCsSO_4$ at different temperatures were investigated. For correlation and definite identification of the spectral features, its infrared absorption spectrum was also studied. An analysis of the intensities and polarizations of the internal modes of the sulphate ions reveals the change in symmetry of the crystal. The integrated intensity and peak height of the ν_1 line, plotted against temperature show anomalous peaks in the region of the phase transition. Differential scanning calorimetric study gives the enthalpy change ΔH across the phase transition to be 0.213 kJ/mol.

Keywords. Ferroelastic; structural phase transition; total integrated intensity; fluctuations; differential scanning calorimetry.

PACS No. 78·30

1. Introduction

$LiCsSO_4$ belongs to a large family of crystals with the general formula $M'M''SO_4$ (M', $M'' = Li^+, K^+, Cs^+, Rb^+$). This crystal undergoes a phase transition at 202 K from the room temperature orthorhombic *P cmn* phase to a low temperature ferroelastic phase of $P2_1/n$ symmetry. X-ray structural studies (Kruglik *et al* 1979) revealed that the principal structural change across the phase transition is that the SO_4 tetrahedra rotate about the orthorhombic *c*-axis through 14°. Aleksandrov *et al* (1980) and Delfino *et al* (1980) studied the thermal and dielectric properties of this crystal. Aleksandrov *et al* observed anomalies in the specific heat and in the dielectric constant ε_b at 202°K. The lattice parameters of $LiCsSO_4$ have been measured by Pietraszko *et al* (1981) in both the orthorhombic and monoclinic phases. In their optical measurements, Pietraszko *et al* have also observed very thin domains just below the phase transition point. The elastic constants C_{ij} were measured by Aleksandrov *et al* (1981) at various temperatures above T_c. Some of the elastic constants showed anomalies near the phase transition. Recently, Pakulski *et al* (1983) observed stress-strain hysteresis loops at various temperatures in the ferroelastic phase. This paper presents the Raman spectroscopic investigations of the phase transition in $LiCsSO_4$.

2. Experimental

A 1:1 mixture of Li_2SO_4 and Cs_2SO_4 was used to prepare the aqueous solution. Single crystals of $LiCsSO_4$ that were obtained were colourless. A parallelpiped ($2 \times 3 \times 4$ mm) with its faces perpendicular to the *a*, *b* and *c* axes was cut from a good single crystal.

A Spex Ramalog double monochromator spectrometer with a photon counting detection system was used to record the Raman spectra. The 4880 Å line from a Spectra-Physics Argon laser with a power of 250 mW was used to excite the Raman spectra. The slit width employed corresponds to a spectral resolution of $3.5\,cm^{-1}$.

The IR spectrum of $LiCsSO_4$ was recorded in nujol mull at room temperature using a Perkin Elmer IR spectrometer (Model 580) with a resolution of $3\,cm^{-1}$.

3. Results and discussion

$LiCsSO_4$ crystallises in the orthorhombic system with the space group *Pcmn* (D_{2h}^{16}) and the lattice constants are $a = 9{\cdot}456$Å, $b = 5{\cdot}456$Å and $c = 8{\cdot}820$Å. The primitive unit cell contains four formula units. In the unit cell the SO_4^{2-}, Li^+ and Cs^+ ions occupy C_s sites. In our analysis of the polarised spectra, the laboratory coordinate system of *x*, *y*, *z* axes are identified with the crystallographic axes *a*, *b*, *c* respectively.

The mirror in the *xz* plane that is present in the orthorhombic phase is lost in the monoclinic phase and all the cations and anions occupy C_1 sites in the monoclinic phase. The number of formula units remains the same ($Z = 4$) as in the room temperature phase.

Application of factor group analysis gives the nature of the $k = 0$ vibrational modes and their distribution among the irreducible representations of the factor groups D_{2h} and C_{2h}. In this analysis, the SO_4 groups were treated as single entities in computing the translational (T') and rotational (R') modes. The results are presented in tables 1a and 1b. The correlation between the molecular, site and factor group modes in the two phases are presented in tables 2a and 2b.

(a) *External modes*

In the room temperature phase, group theory predicts $7A_g$, $5B_{1g}$, $7B_{2g}$ and $5B_{3g}$ external modes to be active in the Raman spectrum. Considerably smaller number of modes have been observed. The frequencies and assignment of the external modes observed are presented in table 3 and the polarised spectra in figures 1a and 1b.

(b) *Internal modes*

In a free SO_4 ion, there are four normal modes of vibration; ν_1 (non-degenerate), ν_2 (doubly degenerate), ν_3 and ν_4 (both triply degenerate). These internal modes of the free SO_4 ion are site and/or factor group split in the crystalline state and so there are no degeneracies. The frequencies of the observed internal modes in various settings of the crystal are given in table 3 and the polarised spectra are shown in figures 2a and 2b.

ν_1 modes: We see from the correlation diagram that two modes of A_g and B_{2g} symmetry species are Raman active. We observed a very strong line at $1018\,cm^{-1}$ in the A_g symmetry. In the B_{2g} symmetry also we have observed a strong line at $1018\,cm^{-1}$. In the other two $c(ba)b(B_{1g})$ and $c(bc)b(B_{3g})$ settings, due to the polarisation leakage and also due to slight misalignment of the crystal, we observed weak ν_1 modes at $1018\,cm^{-1}$.

Table 1a. Factor group analysis of $LiCsSO_4$ crystal in the D_{2h} phase.

Symmetry species	N	T	T'	R'	n	Activities
A_g	13	0	6	1	6	x^2, y^2, z^2
B_{1g}	8	0	3	2	3	xy
B_{2g}	13	0	6	1	6	xz
B_{3g}	8	0	3	2	3	yz
A_u	8	0	3	2	3	
B_{1u}	13	1	5	1	6	z
B_{2u}	8	1	2	2	3	y
B_{3u}	13	1	5	1	6	x

Table 1b. Factor group analysis of $LiCsSO_4$ in the C_{2h} phase.

Symmetry species	N	T	T'	R'	n	Activities
A_g	21	0	9	3	9	x^2, y^2, z^2, xy
B_g	21	0	9	3	9	xz, yz
A_u	21	1	8	3	9	
B_u	21	2	7	3	9	

Here N is the total number of degrees of freedom, T the acoustic modes, T' the translatory lattice modes, R' the rotatory lattice modes, n the internal vibrational modes of SO_4^{2-} ions.

Table 2a. Correlation diagram for the free, site and unit cell symmetry of SO_4 ions in $LiCsSO_4$ crystal in the orthorhombic phase.

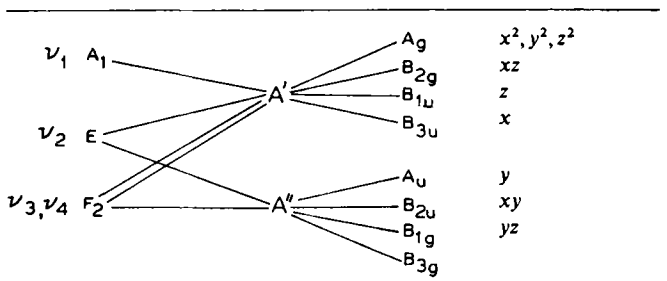

Table 2b. Correlation diagram for the free, site and unit cell symmetry of SO_4 ions in the monoclinic phase.

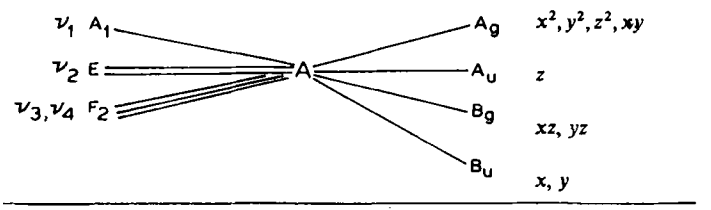

Table 3. Raman frequencies observed in $LiCsSO_4$ crystal in six polarisation settings at room temperature.

Symmetry species	External modes (cm^{-1})	Internal modes (cm^{-1})			
		ν_1	ν_2	ν_3	ν_4
$A_g c(aa)b$	57	1018	450	1124	628
	115			1158	650
$A_g a(bb)c$	56	1018	453	1112	630
	112			1162	654
$A_g a(cc)b$	57	1018	457	1125	625
	145			1159	650
$B_{1g} c(ba)b$	58		460	1110	620
	88				
	118				
$B_{2g} c(ac)b$	58	1018	454	1160	624
	114			1202	652
	150				
$B_{3g} c(bc)b$	58		464	1110	622
	114			1160	654

ν_2 modes: Referring to the correlation table 2a, there are four ν_2 modes of A_g, B_{1g}, B_{2g} and B_{3g} species that are active in the Raman spectrum. All these vibrational modes are observed in the spectrum.

ν_3 modes: All the six ν_3 modes predicted ($2A_g$, $2B_{2g}$, $1B_{1g}$, $1B_{3g}$) from the group theory are observed in the Raman spectrum.

ν_4 modes: Here also, all the six expected ν_4 modes ($2A_g$, $2B_{2g}$, $1B_{1g}$, $1B_{3g}$) have been observed in the Raman spectrum. In the $c(aa)b(A_g)$ setting, the intensity of the line at $628\,cm^{-1}$ is greater than that at $650\,cm^{-1}$ ($I_{628} > I_{650}$). In the $A_g(bb)$ setting also we notice that the line intensity at $630\,cm^{-1}$ is more than that at $654\,cm^{-1}$. But in the

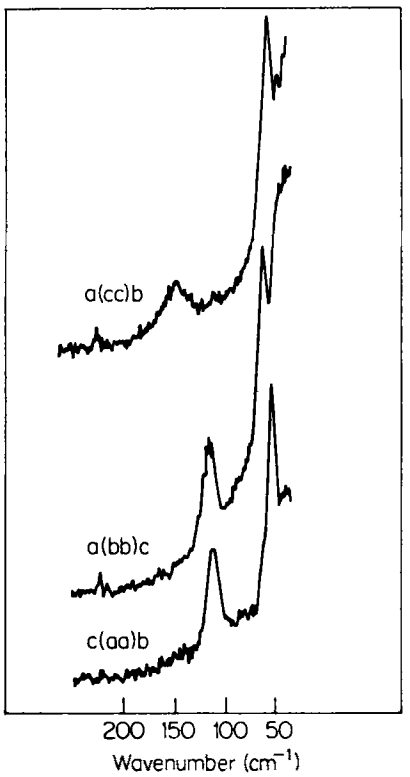

Figure 1a. External modes observed with three on-diagonal settings.

$A_g(cc)$ setting we note that the line intensity at $626\,cm^{-1}$ is smaller than that at $650\,cm^{-1}$.

3. *Low temperature monoclinic phase*

The phase transition at 202 K results in the loss of the mirror plane that is perpendicular to the *b*-axis in the room temperature phase. In this low temperature monoclinic phase, all the Li^+, Cs^+ and SO_4^{2-} ions are on C_1 sites. According to group theory, $12A_g + 12B_g$ external modes and $9A_g + 9B_g$ internal modes are present in the Raman spectrum.

In the low temperature phase in the $c(aa)b\,(A_g)$ setting $7A_g$ external modes have been observed as shown in figure 3. This figure also shows the external modes recorded at room temperature in the $c(aa)b$ polarisation. It is clear that there are $7A_g$ lattice modes at 105 K in the monoclinic phase and $2A_g$ lattice modes at room temperature orthorhombic phase.

The lattice modes were recorded in the $c(ba)b$ setting at 105 K and $4A_g$ modes are present in the spectrum. In the room temperature phase $3B_{1g}$ lattice modes have been observed in the $c(ba)b$ setting.

The internal modes of SO_4^{2-} ions have been recorded at low temperatures in the monoclinic phase in $c(aa)b$ and $c(ba)b$ polarisations. The observed spectra are

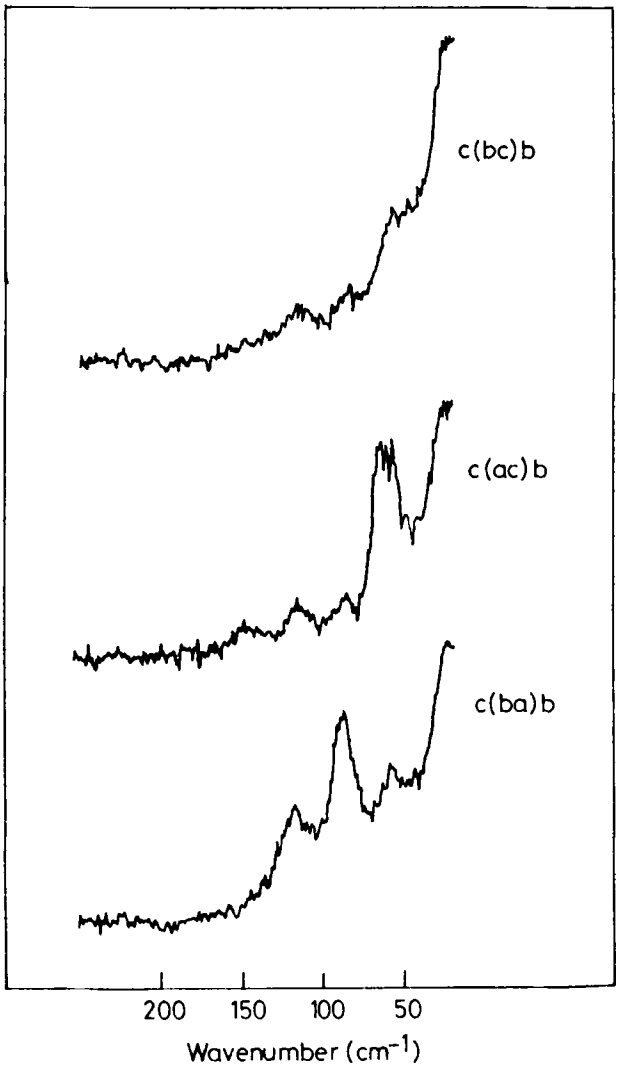

Figure 1b. External modes observed with three off-diagonal settings.

reproduced in figure 4. In the low temperature $c(aa)b$ spectrum, two $\nu_2\,(A_g)$ modes at 456 cm^{-1}, 470 cm^{-1} and three $\nu_4\,(A_g)$ modes at 623 cm^{-1}, 632 cm^{-1} and 656 cm^{-1} are observed. Three $\nu_3\,(A_g)$ modes are observed at 1113 cm^{-1}, 1128 cm^{-1} and 1164 cm^{-1}. Similarly, in the $c(ba)b$ polarisation two $\nu_2\,(A_g)$ modes, three each of $\nu_3\,(A_g)$ and $\nu_4\,(A_g)$ modes are observed. These observations agree with the predictions of the correlation diagram (table 2b). The frequencies and assignment of the external and internal modes in the low-temperature phase are given in table 4. Our Raman spectroscopic results in both the phases of the $LiCsSO_4$ crystal match reasonably well with the group theoretical predictions based on the factor group symmetries of the two phases.

We measured the total integrated intensity of the ν_1 mode in two polarisation settings $c(aa)b$ and $c(ac)b$ at various temperatures across the phase transition. In both the

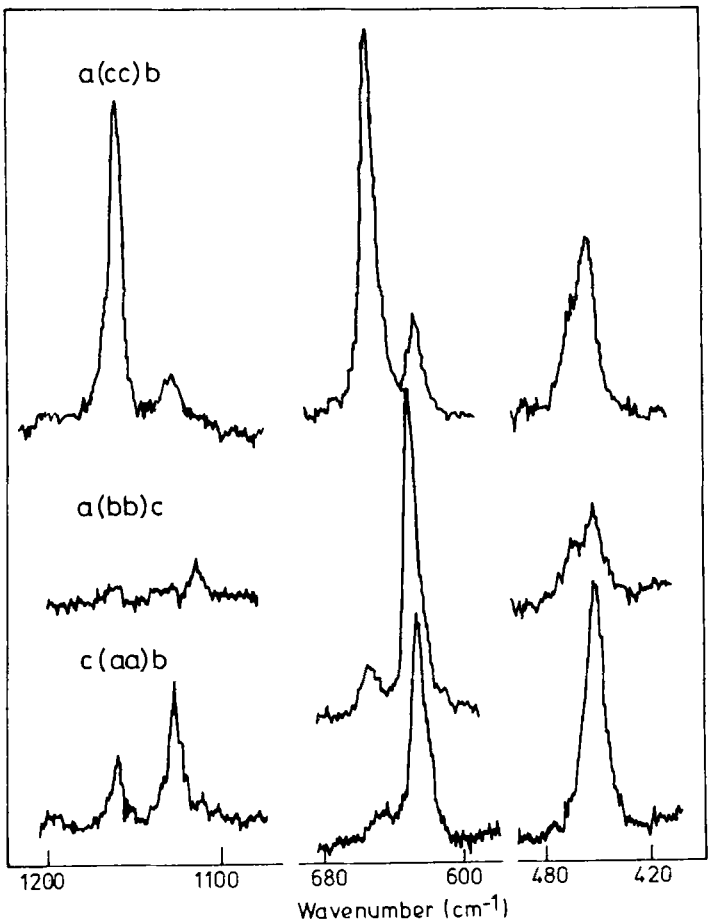

Figure 2a. Internal modes of LCS observed with three on-diagonal settings.

polarisation settings, the total integrated area of the ν_1 mode showed anomalous increase at the phase transition. The intensities of the ν_1 lines under two polarisation settings were added up and plotted against temperature. This addition of areas was done because there are four SO_4 groups in the unit cell and an analysis of their individual tensor components in the crystallographic directions was not easy to carry out. Figure 5 shows the total intensity ($aa + ac$) and line height of the ν_1 line plotted against temperature. As can be clearly seen from this plot the total intensity is temperature dependent and exhibits an anomaly across the phase transition. This anomaly can be attributed to the increase of fluctuations in the polarisability of the scattering species near the phase transition. The linewidth of the ν_1 mode in (aa) and (ac) polarisations plotted against temperature is shown in figure 6. However, the linewidth does not show any anomalous behaviour at the phase transition.

The IR absorption spectrum of $LiCsSO_4$ was recorded at room temperature covering the internal vibrations of SO_4 ions. Group theory gives 6 $(B_{1u} + B_{3u}) + 3B_{2u}$ modes of

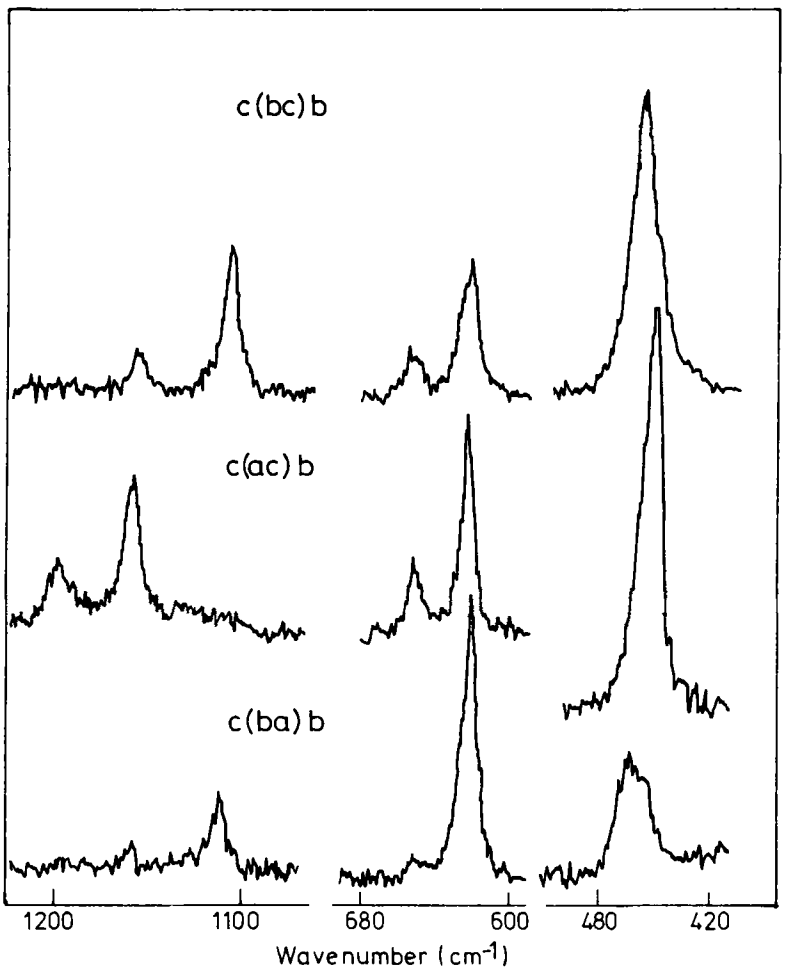

Figure 2b. Internal modes of LCS observed with three off-diagonal settings.

internal vibrations to be active in the IR spectrum. The IR spectrum is shown in figure 7 and the identification of the bands also is given in the same figure.

This crystal has also been studied through differential scanning calorimetry using a Perkin Elmer DSC-2 differential scanning calorimeter. Heating rate employed was 10°K/min and the intensity used was 1 m cal/sec. The DSC thermogram shown in figure 8 has one endothermic peak at 201°K during the heating. From the DSC curve, the change in enthalpy at the phase transition is found to be 0·213 kJ/mol.

It is interesting to make a comparative study of the enthalpies involved at the phase transitions in $LiCsSO_4$, Cs_2CdBr_4, $(N(CH_3)_4)_2\ ZnBr_4$ (Perret *et al* 1983) and $LiRbSO_4$ (Shiroishi and Sawada 1979) wherein the phase transitions involve rotation of the tetrahedral species present in them. Cs_2CdBr_4 undergoes a phase transition from *P mna* to $P2_1/n\ 11$ *via* an incommensurate phase and the main structural change across the phase transition is the rotation of the $CdBr_4$ tetrahedra (Plesko *et al* 1980) around the *x*-axis. The transition enthalpy was reported to be $\Delta H = 0{\cdot}15$ kJ/mol which is

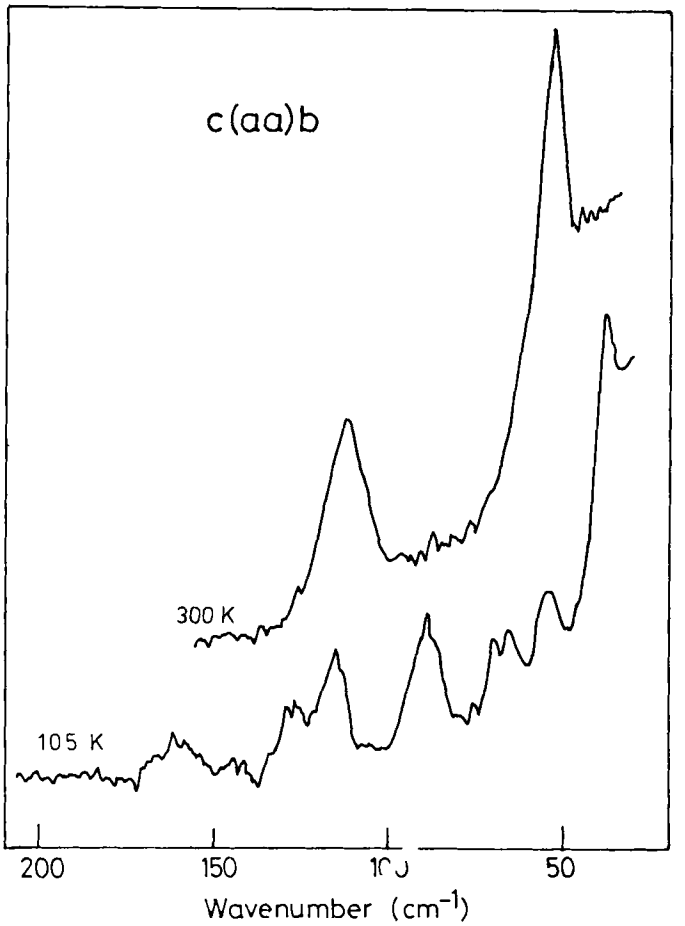

Figure 3. External modes of LCS in the *c(aa)b* setting at 300 K and 105 K.

Table 4. Raman frequencies observed in $LiCsSO_4$ in two polarisation settings at 105 K.

Symmetry species	External modes (cm^{-1})	Internal modes (cm^{-1})			
		ν_1	ν_2	ν_3	ν_4
$A_g c(aa)b$	39	1020	456	1113	623
	55		470	1128	632
	66			1164	656
	90				
	116				
	127				
	160				
$A_g c(ba)b$	41	1021	456	1116	623
	60		470	1130	630
	86			1163	655
	114				

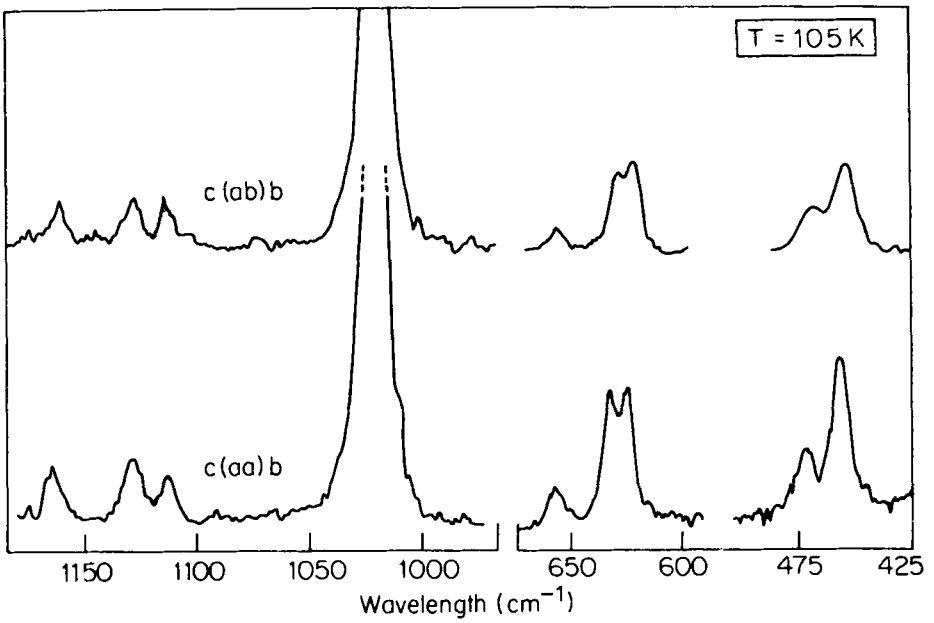

Figure 4. Raman spectra of LCS in two polarisation settings covering the internal mode region at 105 K.

comparable with that observed in $LiCsSO_4$. Another system $(N(CH_3)_4)_2ZnBr_4$ showing a phase transition between $P\,mna$ and $P2_1/n$ 11 phases also involves rotation of the $ZnBr_4$ tetrahedra around the x- and z- axes. The transition enthalpy $\Delta H = 2.35$ kJ/mol is much more than that involved in $LiCsSO_4$ and Cs_2CdBr_4 crystals. Perret *et al* (1983) have attributed this large value of enthalpy to the thermal motions of the methyl groups. The $LiRbSO_4$ crystal shows successive phase transitions at 166, 185, 202 and 204°C and the crystal symmetries in various phases are $P\,112_1/n$ ($T < 166$°C), $P\,11\,n$ ($166 < T < 185$°C), $P2_1/c\;11$ ($185 < T < 202$°C) and $P\,mcn$ ($T > 204$°C). The transition enthalpies involved are 0·083 kJ/mol (at 166°C), 0·012 kJ/mol (at 185°C), 0·544 kJ/mol (at 202°C) and 0·334 kJ/mol (at 204°C). It can be seen that, except the enthalpy value at 204°C, the other three values in $LiRbSO_4$ differ considerably from the enthalpy change observed in $LiCsSO_4$.

From our results, it is clear that the Raman spectra in both the phases of $LiCsSO_4$ crystal agree well with the group theoretical predictions. The peak height and integrated intensity of the totally symmetric line show anomalous increase near the phase transition.

Further Raman spectroscopic study and the dielectric constant measurements under high pressures are in progress to get a better understanding of the structural changes that take place across the ferroelastic phase transition.

Acknowledgements

The authors thank the DST for financial support for the Spex Raman Spectrometor. One of the authors (BRC) thanks the DAE for the financial support.

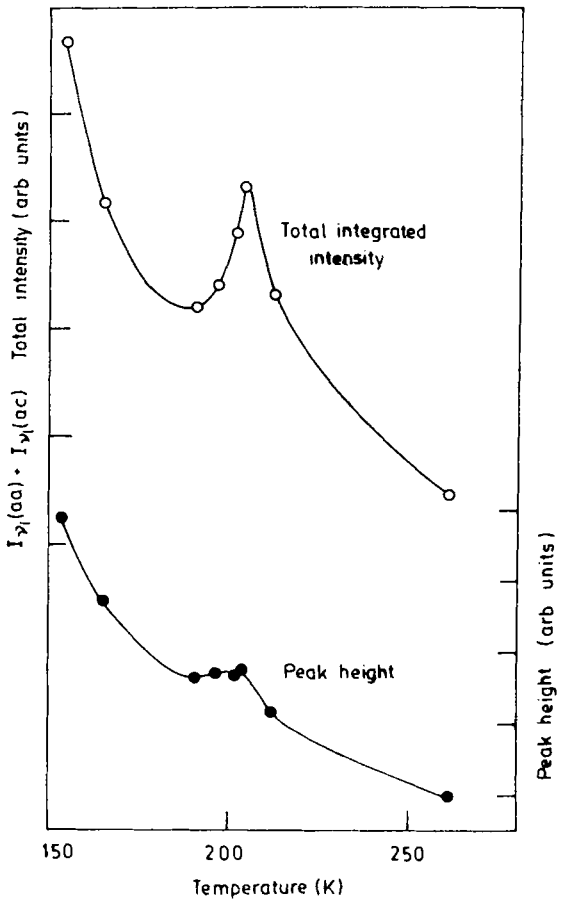

Figure 5. Plots of intensity and peak height of the totally symmetric stretching mode against temperature.

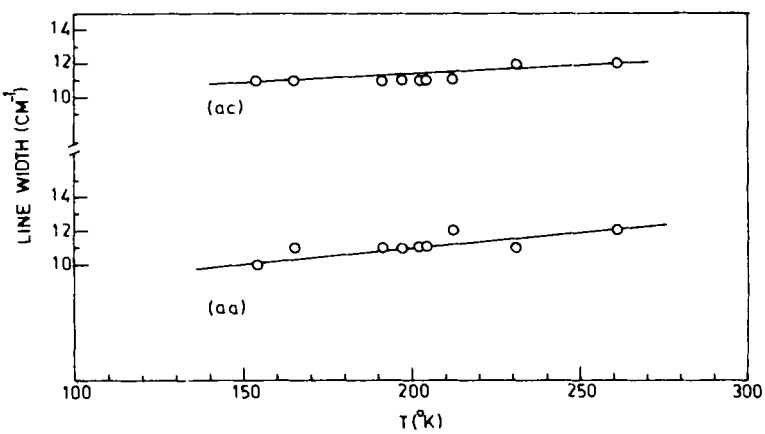

Figure 6. Linewidth variation of ν_1 mode in *aa* and *ac* settings across the phase transition.

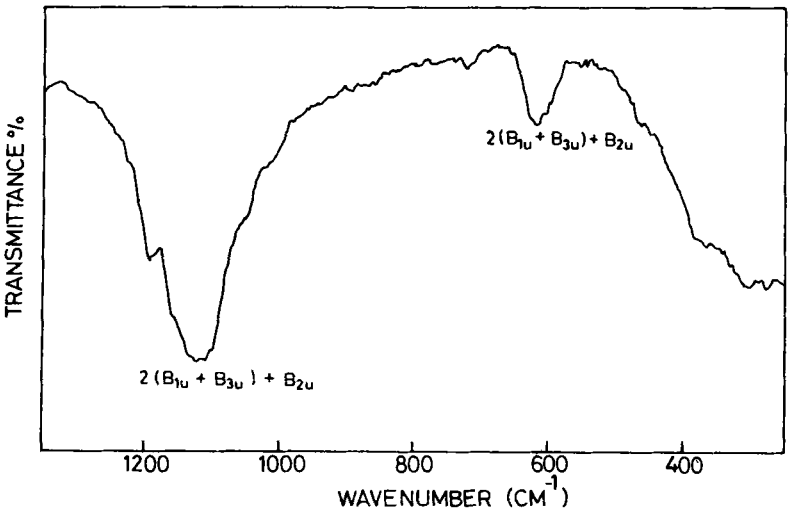

Figure 7. IR absorption spectrum of LCS recorded in mull at room temperature.

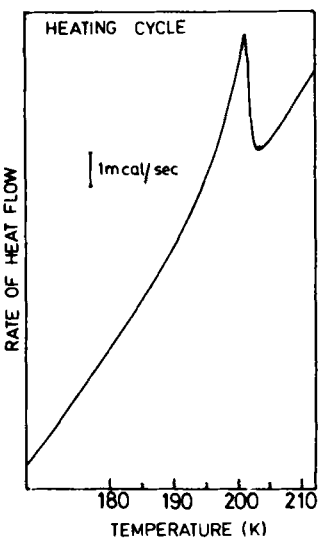

Figure 8. Typical DSC anomaly of $LiCsSO_4$.

References

Aleksandrov K S, Zhereotsova L I, Iskornev I M, Kruglik A I, Rozanov O V and Flerov I N 1980 *Sov. Phy. Solid State* **22** 2150

Aleksandrov K S, Zafsova M P, Shabanova L A and Shimanaskaya O V 1981 *Fiz. Tverd. Tela* **23** 2440

Delfino M, Loiacano G M, Smith W A, Shaulov A, Tsuo Y H and Bell M I 1980 *J. Solid State Chem.* **31** 131
Kruglik A I, Simonov M A, Zhelezin E P and Belov N V 1979 *Sov. Phy. Dokl.* **24** 596
Pakulski G, Mroz B and Krajewski T 1983 *Ferroelectrics* **48** 259
Perret R, Beaucamps Y, Godefroy G, Muralt P, Ehreusperger M, Arend H and Altermatt D 1983 *J. Phys. Soc. Jpn* **52** 2523
Pietraszko A, Tomaszewski P E and Lukaszewicz K 1981 *Phase Transitions* **2** 141
Plesko S, Kind R and Arend H 1980 *Ferroelectrics* **26** 703
Shiroishi Y and Sawada S 1979 *J. Phys. Soc. Jpn* **46** 148